修士論文要旨 (2013 年度)

# 等価電磁流法による 誘電体からの散乱について

On the Scattering From Dielectric Bodies Using Equivalent Current Method

電気電子情報通信工学専攻　ヌエン　ヌゴック　アン
Nguyen Ngoc An

## 1. Introduction

In recent several decades, topics on electromagnetics scattering have been widely studied with several target shapes and models using rigorous analytical calculation in some cases and approximations in other cases. Exact solution is desirable everywhere, however, it is not always possible to obtain exact solution for a problem.

Besides, asymptotic high frequency methods provides powerful and fast ability in analysing a wide variety of electromagnetic scattering problems of electrically large objects [1] [2].

Among high frequency methods, Kirchhoff approximation is a powerful group of methods that has been under study for several years. A well-known member of this group is the Physical Optics (PO). This conventional PO is based on surface electric current excited by incident wave. Several efforts were contributed to improve the methods. For example, Kobayashi and his colleagues offered an extended version of the PO and treated the scattering from impedance surface [4]. Yet, this method is still limited to metallic surface and has certain defects. One good point of the process in PO is the use of equivalent current. Not like in the approach in ray optics, which requires attention on any possible ray path, or in the approach of of numerical methods like Finite Difference Time Domain method with a large amount of calculation, the equivalent current method help one calculate speedily scattering field by direct integration of the current over the scattering body.

This thesis is an effort to obtain a 3D solution for scattering from dieletric surfaces, from which one can make further analysis for other information of the target. Awared of the merits of the equivalent current method, the thesis proposes and uses a modification of the equivalent currents which are, now, based on the reflected wave. The currents consist of electric and magnetic currents flowing on a hypothetical plane. This makes the method applicable on even dielectric surface.

## 2. Scattering from a surface - 2D problem

The problem will be first formulated on a two dimensional surface with the incidence of a transverse magnetic polarized plane wave to a surface AB as depicted in Fig.1. $\theta_0$ is the incident angle. The medium above AB

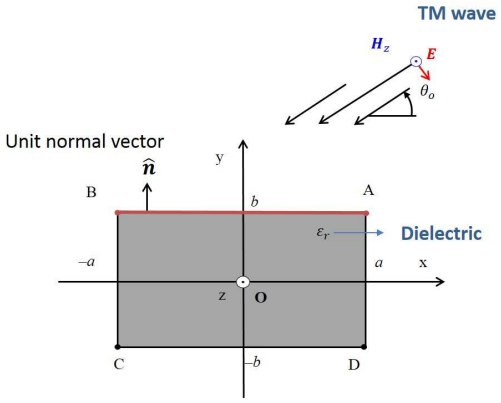


Figure 1: Scattering from a dielectric surface

is free space, while the lower part has relative permittivity $\epsilon = \epsilon_0\epsilon_r$. A Cartesian and a cylindrical coordinates are set up at the center of the surface. Here, the time harmonic factor $e^{-i\omega t}$ is used, but suppressed throughout the context. Then the incident wave will take the following forms:

$$H_z^i = e^{-ik_0 x\cos\theta_0 - ik_0 y\sin\theta_0}, \tag{1}$$

$$E_x^i = \sqrt{\frac{\mu_0}{\epsilon_0}}\sin\theta_0 e^{-ik_0 x\cos\theta_0 - ik_0 y\sin\theta_0}, \tag{2}$$

$$E_y^i = -\sqrt{\frac{\mu_0}{\epsilon_0}}\cos\theta_0 e^{-ik_0 x\cos\theta_0 - ik_0 y\sin\theta_0}. \tag{3}$$

Fig.2 depicts the assumption that the surface AB of the dielectric body belongs to an infinite surface of the same nature. Consequently, reflections at both ends of the surface are similar to reflection else where on the

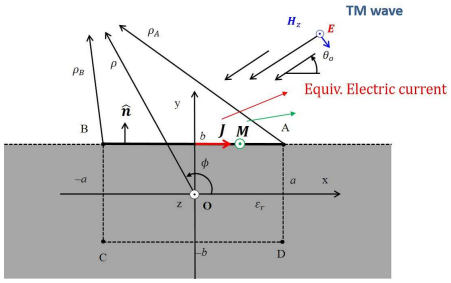


Figure 2: Equivalent currents

surface. The reflected wave is given by the following form:

$$H_z^r = \Gamma^{TM}(\theta_0)e^{-ik_0x\cos\theta_0+ik_0y\sin\theta_0}, \quad (4)$$

$$E_x^r = -\sqrt{\frac{\mu_0}{\epsilon_0}}\sin\theta_0\Gamma^{TM}(\theta_0)e^{-ik_0x\cos\theta_0+ik_0y\sin\theta_0}, \quad (5)$$

$$E_y^r = -\sqrt{\frac{\mu_0}{\epsilon_0}}\cos\theta_0\Gamma^{TM}(\theta_0)e^{-ik_0x\cos\theta_0+ik_0y\sin\theta_0}. \quad (6)$$

Here, $\Gamma^{TM}(\theta_0)$ is the reflection coefficient. On the surface AB, $\Gamma^{TM}(\theta_0)$ can be calculated by

$$\Gamma^{TM}(\theta_0) = \frac{\epsilon_r\sin\theta_0 - \sqrt{\epsilon_r - \cos^2\theta_0}}{\epsilon_r\sin\theta_0 + \sqrt{\epsilon_r - \cos^2\theta_0}}. \quad (7)$$

On surface $y = b$ with $-a \le x \le a$, assume that there are magnetic current $\boldsymbol{M}$ and electric current $\boldsymbol{J}$ are described by the following equations:

$$\boldsymbol{J} = H_z^r\hat{\boldsymbol{x}} = \Gamma^{TM}(\theta_0)e^{-ik_0x\cos\theta_0}\hat{\boldsymbol{x}}, \quad (8)$$

$$\boldsymbol{M} = E_x^r\hat{\boldsymbol{z}} = -\sqrt{\frac{\mu_0}{\epsilon_0}}\sin\theta_0\Gamma^{TM}(\theta_0)e^{-ik_0x\cos\theta_0}\hat{\boldsymbol{z}}. \quad (9)$$

From the Maxwell's equations, one can establish wave equations.

$$\nabla^2\boldsymbol{A} + k_0^2\boldsymbol{A} = -\mu_0\boldsymbol{J}, \qquad \nabla^2\boldsymbol{F} + k_0^2\boldsymbol{F} = -\epsilon_0\boldsymbol{M} \quad (10)$$

Based on which the scattering farfield can be derived.

$$\mu_0\boldsymbol{H} = \nabla\times\boldsymbol{A} + i\omega_0\mu_0\boldsymbol{F} - \frac{1}{i\omega_0\epsilon_0}\nabla(\nabla\cdot\boldsymbol{F}) \quad (11)$$

In the upper half plane ($y >$b), one may get

$$H_z^s = -\frac{i}{4}\int_{-a}^{a} J_x(x_0)\frac{\partial}{\partial y}H_0^{(1)}(\chi)\Big|_{y_0=b}dx_0 - \frac{\omega_0\epsilon_0}{4}\int_{-a}^{a} M_z(x_0)H_0^{(1)}(\chi)\Big|_{y_0=b}dx_0, \quad (12)$$

where $\chi = k_0\sqrt{(x-x_0)^2+(y-y_0)^2}$, and $H_0^{(1)}(\chi)$ denotes the zero-th order Hankel function of the first kind. Spectral representation of this Hankel function is given by

$$H_0^{(1)}(x,y,x_0,y_0) = \int_{-\infty}^{\infty}\frac{e^{i\xi(x-x_0)+i\sqrt{k_0^2-\xi^2}|y-y_0|}}{\pi\sqrt{k_0^2-\xi^2}}d\xi. \quad (13)$$

When one applies the Saddle Point Method to the the integral for farfield, there is a pole singularity at $\xi = -k\cos\theta_0$, whose residue recovers the reflected wave. Meanwhile, each saddle point contribution gives us diffracted field. For the backscattering farfield, contribution from the saddle points become dominant. Thus, the backscattering farfield can be represented by

$$H_z^{'s}(\rho,\phi) = (-2i)\frac{e^{ik_0\rho+i\pi/4}}{2\sqrt{2\pi k_0\rho}}\frac{\sin\phi+\sin\theta_0}{\cos\phi+\cos\theta_0}\Gamma^{TM}(\theta_0) \cdot e^{-i2k_0b(\sin\theta_0+\sin\phi)} \cdot\sin[k_0a(\cos\phi+\cos\theta_0)], \quad (14)$$

where $(\rho,\phi)$ denotes the cylindrical coordinate as in Fig.2.

# 3. 3D extension of the problem

## 3.1 General treatment

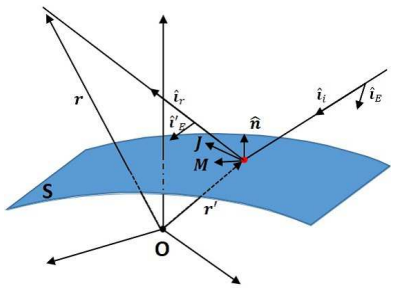


Figure 3: Scattering from surface S

Let's consider a general surface of relative permittivity $\epsilon_r$ being illuminated by an incident wave as illustrated in Fig.3. The incident wave is defined by an unit propagation vector $\hat{\boldsymbol{i}}_i$ and an unit direction vector of the electric field $\hat{\boldsymbol{i}}_E$. Similarly the reflected wave is defined by $\hat{\boldsymbol{i}}_r$ and $\hat{\boldsymbol{i}}'_E$ according to the Snell's law of reflection. $\hat{\boldsymbol{n}}$, $\boldsymbol{J}$ and $\boldsymbol{M}$ are the unit normal vector, electric equivalent current and magnetic equivalent current at the point of reflection respectively. $\boldsymbol{r'}$ is the displacement vector of the current and $\boldsymbol{r}$ points from the origin to the observation point at infinity. Vector potentials $\boldsymbol{A}$ and $\boldsymbol{F}$ can be represented using 3D Green function.

$$\boldsymbol{F} = \epsilon_0\int_S \boldsymbol{M}(\boldsymbol{r'})\frac{e^{ik|\boldsymbol{r}-\boldsymbol{r'}|}}{4\pi|\boldsymbol{r}-\boldsymbol{r'}|}dS \quad (15)$$

$$\boldsymbol{A} = \mu_0\int_S \boldsymbol{J}(\boldsymbol{r'})\frac{e^{ik|\boldsymbol{r}-\boldsymbol{r'}|}}{4\pi|\boldsymbol{r}-\boldsymbol{r'}|}dS \quad (16)$$

Then the scattering farfield can be calculated by

$$\mu_0\boldsymbol{H} = \nabla\times\boldsymbol{A} + i\omega_0\mu_0\boldsymbol{F} - \frac{1}{i\omega_0\epsilon_0}\nabla(\nabla\cdot\boldsymbol{F}), \quad (17)$$

$$\epsilon_0\boldsymbol{E} = -\nabla\times\boldsymbol{F} + i\omega_0\epsilon_0\boldsymbol{A} - \frac{1}{i\omega_0\mu_0}\nabla(\nabla\cdot\boldsymbol{A}). \quad (18)$$

## 3.2 Application to dielectric slab

The case of a TE incidence to a dielectric slab is depicted in Fig.4. One may notice that an arbitrarily linear polarized wave can be well disintegrated to transverse electric and transver magnetic components. Furthermore, these two components can be treated in a similar manner. In this resume, the formulation will be proceeded for TE wave. Solution for TM wave can be found in the thesis.

As shown in Fig.4, the coming wave impinges the surface at elevation angle $\theta_0$ and azimuth angle $\phi_0$. Others vectorial notions are the same as explained in the general case above.

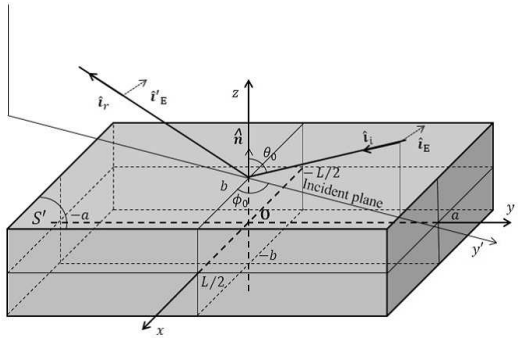


Figure 4: Scattering from a dieletric slab

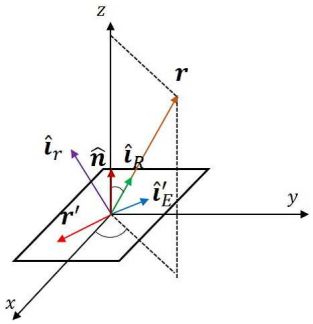


Figure 5: Scattering from a dieletric slab

$$\hat{\boldsymbol{n}} = (0,0,1)$$
$$\hat{\boldsymbol{i}}_i = (-\sin\theta_0\cos\phi_0, -\sin\theta_0\sin\phi_0, -\cos\theta_0)$$
$$\hat{\boldsymbol{i}}_r = \hat{\boldsymbol{i}}_i - 2\hat{\boldsymbol{n}}(\hat{\boldsymbol{i}}_i \cdot \hat{\boldsymbol{n}})$$
$$\hat{\boldsymbol{i}}_E = \hat{\boldsymbol{i}}'_E = (-\sin\phi_0, \cos\phi_0, 0)$$

Beside the Cartesian coordinate, one local spherical coordinate is also located at the origin O as in Fig.5.

$$\hat{\boldsymbol{i}}_R = (\sin\theta\cos\phi, \sin\theta\sin\phi, \cos\theta)$$
$$\hat{\boldsymbol{i}}_\theta = (-\cos\theta\cos\phi, -\cos\theta\sin\phi, -\sin\theta)$$
$$\hat{\boldsymbol{i}}_\phi = (-\sin\phi, \cos\phi, 0)$$

The incident and reflected fields can be represented by

$$\boldsymbol{E}_i = E_0\hat{\boldsymbol{i}}_E e^{ik_0\hat{\boldsymbol{i}}_i\cdot\boldsymbol{r}},$$
$$\boldsymbol{E}_r = \Gamma(\theta_0)E_0\hat{\boldsymbol{i}}'_E e^{ik_0 2b\cos\theta_0} e^{ik_0\hat{\boldsymbol{i}}_r\cdot\boldsymbol{r}},$$
$$\boldsymbol{H}_r = \frac{1}{Z_0}\Gamma(\theta_0)E_0(\hat{\boldsymbol{i}}_r \times \hat{\boldsymbol{i}}'_E)e^{ik_0 2b\cos\theta_0} e^{ik_0\hat{\boldsymbol{i}}_r\cdot\boldsymbol{r}},$$

in which $\Gamma(\theta_0)$ is the reflection coefficient of the surface. Accordingly, equivalent currents are provided by

$$\boldsymbol{J} = \frac{1}{Z_0}\Gamma(\theta_0)E_0\left(\hat{\boldsymbol{n}} \times (\hat{\boldsymbol{i}}_r \times \hat{\boldsymbol{i}}'_E)\right) e^{ik_0 2b\cos\theta_0} e^{ik_0\hat{\boldsymbol{i}}_r\cdot\boldsymbol{r}} \quad (19)$$
$$\boldsymbol{M} = \Gamma(\theta_0)E_0(\hat{\boldsymbol{i}}'_E \times \hat{\boldsymbol{n}})e^{ik_0 2b\cos\theta_0} e^{ik_0\hat{\boldsymbol{i}}_r\cdot\boldsymbol{r}} \quad (20)$$

Explicit formulae for vector potential $\boldsymbol{A}$ and $\boldsymbol{F}$ can be derived.

$$\boldsymbol{A} \approx \mu_0\frac{1}{Z_0}\Gamma(\theta_0)E_0\frac{e^{ik_0 r}}{4\pi r}e^{ik_0 2b\cos\theta_0} \cdot\int_S \left(\hat{\boldsymbol{n}} \times (\hat{\boldsymbol{i}}_r \times \hat{\boldsymbol{i}}'_E)\right) e^{ik_0(\hat{\boldsymbol{i}}_r - \hat{\boldsymbol{i}}_R)\boldsymbol{r}'}ds \quad (21)$$

$$\boldsymbol{F} \approx \epsilon_0\Gamma(\theta_0)E_0\frac{e^{ik_0 r}}{4\pi r}e^{ik_0 2b\cos\theta_0} \cdot\int_S (\hat{\boldsymbol{i}}'_E \times \hat{\boldsymbol{n}})e^{ik_0(\hat{\boldsymbol{i}}_r - \hat{\boldsymbol{i}}_R)\boldsymbol{r}'}ds \quad (22)$$

Because of the plane wave assumption, one can approximate the electric farfield scattering in the spherical coordinate as

$$\epsilon_0\boldsymbol{E} \approx i\omega_0\left(\boldsymbol{A} - \hat{\boldsymbol{i}}_R(\hat{\boldsymbol{i}}_R \cdot \boldsymbol{A}) - Z_0\hat{\boldsymbol{i}}_R \times \boldsymbol{F}\right) \quad (23)$$

Projecting the electric scattering farfield on $\theta$ and $\phi$ axes, one receives these corresponding components.

$$\boldsymbol{E}^\theta = i\omega_0[\boldsymbol{A}.\hat{\boldsymbol{i}}_\theta + Z_0\boldsymbol{F}.\hat{\boldsymbol{i}}_\phi] \quad (24)$$
$$\boldsymbol{E}^\phi = i\omega_0[\boldsymbol{A}.\hat{\boldsymbol{i}}_\phi - Z_0\boldsymbol{F}.\hat{\boldsymbol{i}}_\theta] \quad (25)$$

One substitutes Eqs.(21), (22) into Eqs.(24), (25), then executes the scattering integrals on surface S to have the electric scattering farfield. Because of the limited space, the expressions are suppressed here. Regarding reflection coefficient, the reflection which takes place only at the surface S has the following coefficient for the TE wave.

$$\Gamma(\theta_0) = \frac{\cos\theta_0 - \sqrt{\epsilon_r - \sin^2\theta_0}}{\cos\theta_0 + \sqrt{\epsilon_r - \sin^2\theta_0}} \quad (26)$$

However, the multiple boucing effect inside the slab also needs to be considered. In this current configuration of the dieletric slab sandwiched by air,the multiple reflection coefficients are given by

$$\Gamma_m(\theta_0) = \frac{\Gamma(\theta_0) - \Gamma(\theta_0)e^{i4k_0 b\sqrt{\epsilon_r - \sin\theta_0{}^2}}}{1 - \Gamma^2(\theta_0)e^{i4k_0 b\sqrt{\epsilon_r - \sin\theta_0{}^2}}} \quad (27)$$

# 4. Method Validation and Conclusion

The proposed method is different from the PO at the point that PO use only electric current; meanwhile the proposed solution uses both electric and magnetic currents. This procedure opens the potential use of the method on dielectric surface. Solutions by the two methods for a PEC surface coincide exactly under monostatic condition. However, difference can be observed in bistatic calculation. Around the specular reflection beam, the results by GTD and our method show good agreement. However, our method and the PO are not accurate in bistatic back scattering and both fall near

the grazing angles. See Fig.6. Monostatic RCS measurement of scattering of a TM wave from a metal plate at different frequencies reinforces this conclusion. An example is given in Fig.7.

Monostatic RCS measurements of scattering of a TM wave from dielectric boxes show that the proposed multiple reflection coefficient $\Gamma_m$ explains well the scattering property around specular reflection directions. Around the edge region, the approximation failed to explain the RCS pattern of the boxes. One example is shown in Fig.8.

Fig.9 shows the a comparison of estimated and measured peak RCS of a 100 mm× 40 mm×100 mm dielectric box's large surfaces. The RCS estimations with and without multiple bouncing effect included are represented by the black solid line and the blue dashed line, respectively. The dark olive green dot line and the red dot line show the measured RCS data. The mean RCS values of the two faces is indicated by the dark green line. As can be seen, the RCS estimated with single reflection coefficient express a linear behavior through the frequency range. Meanwhile, the RCS$_m$ shows oscillation in accordance with the measured data.

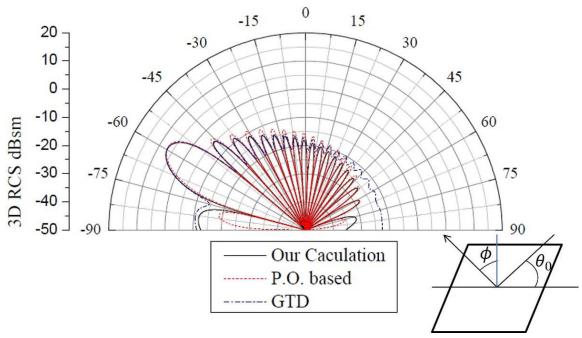


Figure 6: Bistatic RCS of a $10\lambda \times 10\lambda$ metal plate with incident angle $\theta_0 = 30°$

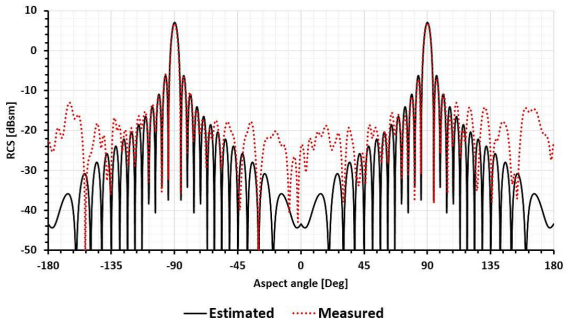


Figure 7: Scattering from a metal plate (100 mm× 100 mm × 0.3 mm) - 19 GHz

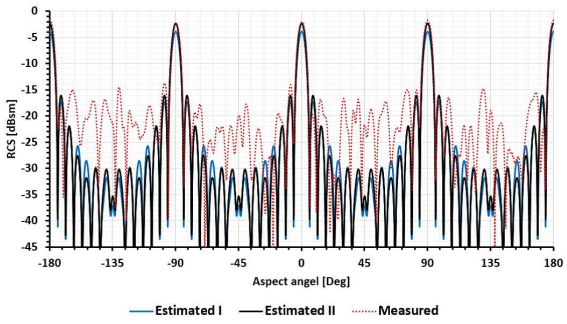


Figure 8: Angular monostatic RCS of a 80 mm× 80 mm×80 mm dielectric box at 19 GHz

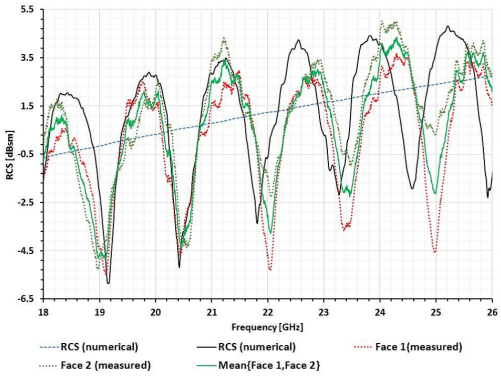


Figure 9: Peak RCS of a 100 mm× 40 mm×100 mm dielectric box's large surfaces with respect to frequency

# References


[1] P. Pathak, "A Summary of Asymptotic High Frequency (HF) Methods for Solving Electromagnetics (EM) Wave Problems", Lecture notes of 2013 International Symposium on Electromagnetic Theory, Hiroshima, Japan.

[2] H. Shirai, "GTD wo kiwameru", Textbook for IEICE-AP Workshop, 2013.

[3] J. B. Keller, "Geometrical Theory of Diffraction," JOSA, Vol. 52, Issue 2, pp. 116-130, 1962.

[4] H.Kobayashi, K Hongo and I. Tanaka, "Expressions of Physical Optics Integral for Smooth Conducting Scatterers Approximated by Quadratic Surfaces,"IEICE Trans. Comm. Vol. J81-B-II, no.9, pp. 863-871, Sep. 1998.

[5] E. F. Knott, J. F. Shaeffer, M. T. Tuley, Radar Cross Section, 2nd ed, Massachusetts, USA: Artech House, 1993.

[6] E. F. Knott, Radar Cross Section Measurements, New York, USA: Van Nostrand Reinhold, 1993.